NASA TECHNICAL NOTE

NASA TN D-7532

NASA TN D-7532

STRAIN-CYCLING FATIGUE BEHAVIOR OF TEN STRUCTURAL METALS TESTED IN LIQUID HELIUM (4 K), IN LIQUID NITROGEN (78 K), AND IN AMBIENT AIR (300 K)

by Alfred J. Nachtigall

Lewis Research Center

Cleveland, Ohio 44135

NATIONAL AERONAUTICS AND SPACE ADMINISTRATION • WASHINGTON, D. C. • FEBRUARY 1974

1. Report No. NASA TN D-7532	2. Government Accession No.	3 ecipient's Catalog No.
4. Title and Subtitle STRAIN-CYCLING FATIGUE BEHAVIOR OF TEN STRUCTURAL METALS TESTED IN LIQUID HELIUM (4 K), IN LIQUID NITROGEN (78 K), AND IN AMBIENT AIR (300 K)		5. Report Date February 1974 6. Performing Organization Code
7. Author(s) Alfred J. Nachtigall		8. Performing Organization Report No. E-7613 10. Work Unit No. 501-21
9 Performing Organization Name and Address Lewis Research Center National Aeronautics and Space Administration Cleveland, Ohio 44135		11. Contract or Grant No. 13. Type of Report and Period Covered Technical Note
12. Sponsoring Agency Name and Address National Aeronautics and Space Administration Washington, D.C. 20546		14. Sponsoring Agency Code
15. Supplementary Notes		

16 Abstract

Strain-cycling fatigue behavior of 10 different structural alloys and metals was investigated in liquid helium (4 K), in liquid nitrogen (78 K), and in ambient air (300 K). At high cyclic lives, fatigue resistance increased with decreasing temperature for all the materials investigated. At low cyclic lives, fatigue resistance generally decreased with decreasing temperature for the materials investigated. Only for Inconel 718 did fatigue resistance increase with decreasing temperature over the entire life range investigated. Comparison of the experimental fatigue behavior with that predicted by the Manson method of universal slopes showed that the fatigue behavior of these materials can be predicted for cryogenic temperatures by using material tensile properties obtained at those same temperatures.

17. Key Words (Suggested by Author(s))	18. Distribution Statement
Cryogenic fatigue; Strain cycling; Low-cycle fatigue; Fatigue life predictions; Mechanical properties; Axial fatigue; Liquid nitrogen; Liquid helium	Unclassified - unlimited Cat. 17

19. Security Classif. (of this report)	20. Security Classif. (of this page)	21. No. of Pages	22 Price*
Unclassified	Unclassified	31	$3.00

* For sale by the National Technical Information Service, Springfield, Virginia 22151

STRAIN-CYCLING FATIGUE BEHAVIOR OF TEN STRUCTURAL METALS TESTED IN LIQUID HELIUM (4 K), IN LIQUID NITROGEN (78 K), AND IN AMBIENT AIR (300 K)

by Alfred J. Nachtigall

Lewis Research Center

SUMMARY

The strain-cycling fatigue behavior of 10 different structural alloys and metals (two aluminum alloys, two titanium alloys, two stainless steels, a maraging steel, a high-nickel alloy, pure nickel, and pure copper) was investigated in liquid helium (4 K), in liquid nitrogen (78 K), and in ambient air at room temperature (300 K). Cylindrical hourglass-shaped specimens were loaded in compression and tension about zero mean strain to produce the desired strain ranges. Tensile properties were also obtained for each material and environmental temperature so that they could be used with the method of universal slopes to predict the fatigue behavior at each temperature.

At high cyclic fatigue lives, fatigue resistance increased with decreasing temperature for all the materials investigated. At low cyclic fatigue lives, fatigue resistance generally decreased with decreasing temperature for the materials investigated. Only for Inconel 718 did the fatigue resistance increase with decreasing temperature over the entire life range investigated. Comparison of experimental fatigue behavior with that predicted by the Manson method of universal slopes showed that the strain-cycling fatigue behavior of these materials at cryogenic temperatures can be predicted with an accuracy comparable to that achieved in earlier investigations conducted at room temperature. Eighty percent of the fatigue data obtained at cryogenic temperatures were predicted within a life factor of 3.

INTRODUCTION

It is well known that cryogenic temperatures can markedly affect the fatigue behavior, as well as the mechanical properties, of structural alloys and metals. Most inves-

tigations of the effect of cryogenic temperatures on the fatigue strength of materials have been conducted under load cycling conditions resulting in high cyclic lives (ref. 1). An earlier fatigue investigation at the NASA Lewis Research Center (ref. 2) was also conducted at cryogenic temperatures under load cycling. The higher loading conditions used in reference 2 resulted in much shorter cyclic lives (low-cycle fatigue). Strain-controlled low-cycle fatigue data on materials at cryogenic temperatures are scarce and limited to liquid nitrogen temperatures (ref. 3).

The high cost and complexity of testing apparatus, as well as the limited availability and high cost of cryogenic fluids, make prediction of fatigue behavior at cryogenic temperatures desirable. Prior to this investigation, no known efforts had been made to do so. However, at room temperature, correlation of strain-controlled low-cycle fatigue data with applied cyclic strain and tensile properties of materials has been extensively verified.

The Manson method of universal slopes was developed for predicting room-temperature fatigue behavior (ref. 4) by utilizing easily obtained tensile properties (ultimate tensile strength, elastic modulus, and ductility). It is reasonable to expect that the method could also be used to predict fatigue behavior at cryogenic temperatures by using the necessary tensile properties obtained at cryogenic temperatures. However, the method correlates cyclic fatigue life with applied cyclic strain (rather than the applied cyclic stress used in most investigations). Therefore, hardly any existing cryogenic fatigue data could be used to determine the validity and suitability of the method of universal slopes for predicting the fatigue behavior of structural materials at cryogenic temperatures.

An experimental investigation was therefore conducted at the NASA Lewis Research Center to obtain strain-controlled low-cycle fatigue data on 10 different structural alloys and metals tested in liquid helium, in liquid nitrogen, and in ambient air. The observed experimental fatigue behavior of these materials could then also be compared with the fatigue behavior predicted by the method of universal slopes. Hence, the mechanical properties necessary for applying the prediction method were also determined for each material and temperature.

The units for physical quantities used in this report are given in the International System of Units (SI); however, measurements during the investigation were made in U.S. customary units. Factors relating these two systems of units are given in reference 5; those pertinent to the present investigation are presented in the appendix.

MATERIALS, APPARATUS, AND TEST PROCEDURE

Materials and Specimens

Most of the materials investigated were considered to have potential use at cryogenic temperatures. They included cyclically strain-hardening materials such as the two stainless steels AISI 304L and AISI 310; the nickel-base alloy Inconel 718; unalloyed nickel 270; and oxygen-free, high-conductivity (OFHC) copper. Also included were cyclically strain-softening materials such as the two aluminum-base alloys 2014-T6 and 2219-T851; the two titanium-base alloys Ti-5Al-2.5Sn and Ti-6Al-4V; and a 300-grade, 18-percent-nickel, maraging steel produced by consumable electrode vacuum melting. The chemical composition of these alloys is given in table I. The condition of each of the materials before they were tested is listed in table II.

Specimens from each material investigated were fabricated from wrought bar stock 2.54 centimeters in diameter, with one exception. The 2219-T851 aluminum specimens were fabricated from extruded bar stock, 2.54 centimeters square. Specimen geometry is shown in figure 1. All specimens had 2.54-centimeter-diameter button heads on each end for attachment to the loading columns. Tensile specimens (fig. 1(a)) had a 2.54-centimeter gage length with a 0.635-centimeter test section diameter. Fatigue specimens (fig. 1(b)) had a shape similar to an hourglass with a minimum test section diameter of 0.635 centimeter. Specimens for determining Poisson's ratio and elastic modulus (fig. 1(c)) had a square test section, 0.897 centimeter on each side and 5.1 centimeters long. The flat faces were desirable for cementing strain gages to them.

Test Apparatus

Tensile tests. - Tensile tests were conducted in ambient air (300 K) and in liquid nitrogen (78 K) with conventional universal testing machines. The cryostat used to contain the liquid nitrogen that surrounded the test specimen during tensile tests was essentially a double-walled vacuum-insulated cylindrical vessel open at the top. The lower loading column entered through the bottom by means of a cryogenic fluid seal. Tensile tests in liquid helium (4 K) were conducted in the cryostat and the closed-loop electrohydraulically actuated testing machine used for conducting fatigue tests in liquid helium (see Fatigue tests). This machine possessed several features that made it suitable for conducting tensile tests. One feature was that the closed-loop command signal from the function generator could be manually triggered to initiate the various waveforms from zero output voltage, going either positive or negative as desired. A second feature was that one of the function generator's selectable waveforms was a linear ramp signal.

This signal could be interrupted at any point on the ramp with a "ramp hold" switch and held at that level until the ramp hold switch was returned to its normal "run" position and the ramp resumed its rise. For these tensile tests, loading was applied by means of the linear ramp signal from the function generator controlling displacement of the loading column at a linear rate with respect to time. The rates varied from 1.0 to 3.8 millimeters per minute depending on the expected elongation of the material tested.

Fatigue tests. - Fatigue tests were conducted in either of two closed-loop electrohydraulically actuated fatigue testing machines. The first machine, shown in figure 2, was designed and built at the Lewis Research Center, for the most part from commercially available components. Its highest practical cycling rate was 1.2 hertz. Its maximum load range was ±9000 newtons.

The second fatigue machine was a commercial model of a closed-loop electrohydraulically actuated fatigue machine capable of a cycling rate of 33 hertz with a hydraulic actuator double-amplitude displacement of 1.22 millimeters. The hydraulic actuator was also capable of developing cyclic load amplitudes of ±9000 newtons.

Each testing machine was equipped with a cryostat specifically designed and built for NASA for this investigation. Although the basic design for the two cryostats was the same, experience with the first cryostat dictated several design improvements in the cryostat used with the second machine, which is illustrated in figure 3. It consisted of a vacuum-tight enclosure (I) that surrounded a cylindrical specimen test chamber (N) whose axis was concentric with the specimen loading axis and the cylindrical vacuum jacket (I). The specimen test chamber contained the cryogenic fluid in which the specimen (O) was immersed during tests. To allow access to the test specimen, the cylindrical specimen chamber parted at the middle of its axial length by means of a circumferential solder seal (G). The lower half of the seal had a circumferential well (or trough) to hold the low-temperature solder, which was melted by an integral electric heater (P) whenever the seal had to be made or broken. The upper and lower loading columns (L) were brought through the opposite ends of the chamber with a double bellows arrangement (Q). The concentric double bellows arrangement allowed opening the two halves of the chamber far enough to install a test specimen. It also allowed relative motion between the upper and lower loading columns during tests without placing loads on the chamber itself.

Split couplings (F) engaged the button head on each end of the specimen to the button head on the end of each loading column in the specimen chamber. All axial clearance between the engaging button heads was taken up by a pair of opposing wedges (H) drawn against each other by means of machine nuts on threaded studs extending from the narrow edge of each wedge through each half of the split coupling.

The radiation shield (J) in the vacuum space between the specimen chamber and the outer vacuum jacket consisted of telescoping copper cylinders attached to the upper and

lower loading columns. When tests were conducted with liquid helium in the specimen chamber, the radiation shield was cooled with liquid nitrogen. The lower cylinder was cooled by liquid nitrogen from the radiation shield reservoir (E) flowing through the coil of copper tubing (K) soldered to its outer surface. The larger diameter copper cylinder in the midsection of the cryostat was fastened by thumbscrews to the underside of the radiation shield reservoir containing liquid nitrogen. It was cooled by conduction through interface contact between its mounting flange and the reservoir. And it could be lowered inside the lower section of the vacuum jacket to allow access to the specimen chamber. The upper inside edge of the radiation shield reservoir was fastened to the upper loading column.

Elastic constants. - The apparatus for determining the elastic modulus and Poisson's ratio in ambient air (300 K) and in liquid nitrogen (78 K) was a deadweight creep machine. Fixed loads were applied to the specimens by placing weights on the weight pan. Applied specimen loads were measured with a load cell and associated equipment. The specimen loading train went through an open-mouth dewar surrounding the specimen, with the lower loading column from the specimen extending through the bottom of the dewar. The dewar could be filled with liquid nitrogen, thus immersing the specimen while load and strain determinations were made for that environmental temperature. The apparatus used for determining the elastic constants in liquid helium was the same cryostat and electrohydraulically actuated testing machine used for conducting tensile and fatigue tests in liquid helium.

Instrumentation. - A tensile extensometer was used to measure the elongation of the specimen's test section between 25.4-millimeter gage marks during the early part of each tensile test. The displacement sensing element was a linear variable differential transformer (LVDT) calibrated for the environmental use temperature. The extensometer used with tensile tests in liquid helium is shown in figure 4.

A diametral extensometer was used to sense the cyclic diameter changes of the minimum test section of specimens during fatigue tests. Figure 5 shows the extensometer mounted on a specimen. Again the displacement sensing element was an LVDT calibrated in the use environment.

The boiling temperature of liquid nitrogen enveloping a test specimen was measured with a calibrated platinum resistor and recorded on a strip-chart recorder. The boiling temperature of liquid helium enveloping a test specimen was measured with a calibrated carbon resistor tied to the specimen test section. Calibrations were traceable to NBS standards.

For Poisson's ratio measurements, dimensional changes due to loading of the specimens for each material were measured with foil strain gages cemented to the flat faces. A strain gage was cemented on each face of one pair of opposite parallel faces with the elements parallel to the specimen loading axis. On the adjacent pair of opposite parallel

faces the elements of the strain gages cemented to each face were normal to the loading axis of the specimen. An additional pair of strain gages was cemented to the faces of a dummy block of the same material that had faces the same width as those of the specimen. The pair of strain gages on the dummy block was used with either pair of gages sensing longitudinal or transverse dimension changes of the specimen. They were connected as a Wheatstone bridge, and strain changes were determined using a commercial strain indicator. The dummy block and its strain gages were placed in the same environment as the specimen used to measure elastic modulus and Poisson's ratio to avoid temperature effects.

Test Procedure

Tensile tests. - Tensile tests were conducted on each material in ambient air at room temperature (approximately 300 K), in liquid nitrogen (78 K), and in liquid helium (4 K). During the initial stages of these tests, plots of load against elongation were obtained on an X-Y plotter. The 0.2-percent-offset yield strength data were obtained from these plots.

Fatigue tests. - Push-pull strain-cycling fatigue tests were conducted with each of the 10 materials in ambient air at room temperature (approximately 300 K), in liquid nitrogen (78 K), and in liquid helium (4 K). Feedback into the electrohydraulic closed-loop system came from the diametral extensometer which was sensing changes in specimen test section diameter as demanded by the servocontroller. Diametral total strain range was determined by the setting of the amplitude of the command signal from the function generator into the servocontroller. The waveform of the command signal was sinusoidal for all fatigue tests. The first cycle of each test was initiated from zero load and strain into the compressive strain amplitude of the total strain range. Strain cycling continued about zero mean strain throughout the test. Cyclic load ranges required to produce the diametral strain ranges demanded of the closed-loop system were measured at regular intervals during the test. The measurements were made electrovisually with the aid of an oscilloscope without interrupting the cycling rate. Cycling rates varied from 0.1 hertz for high strain ranges and short cyclic lives to 10 hertz for low strain ranges and long cyclic lives. For this range of cycling rate and the test temperatures used in this investigation, it was assumed that the effect of cycling rate on fatigue life was insignificant. Plots of load against diametral displacement (hysteresis loops) were obtained on an X-Y plotter for the slower cycling rates (higher strain ranges), which did not exceed the response time of the X-Y plotter.

For long-life fatigue tests, when load and strain cycling were entirely elastic, load control rather than strain control was employed for ease of testing.

Elastic constants. - Determination of elastic modulus and Poisson's ratio for each material and temperature required measurement of longitudinal and transverse strains with each increment of load. Strain data were obtained from at least two increasing-decreasing load histories. Care was taken to avoid exceeding the proportional limit for each material.

DATA ANALYSIS AND FATIGUE LIFE PREDICTIONS

Fatigue Data Analysis

The basic raw data obtained from each test were the cyclic fatigue life, the controlled diametral total strain range, and the applied load range at the half-life. The stress range at the half-life was calculated by using the load range at the half-life with the test cross-sectional area at the start of the test.

The longitudinal elastic strain range was calculated from stress range at half-life and the elastic modulus. Determination of longitudinal plastic strain range was made from the following equation:

$$\Delta\epsilon_p^L = 2\left(\Delta\epsilon_t^D - \mu\,\Delta\epsilon_e^L\right) \tag{1}$$

where

$\Delta\epsilon$ strain range

μ Poisson's ratio

L longitudinal

D diametral

t total

e elastic

p plastic

The longitudinal total strain range is the sum of longitudinal elastic and plastic strain ranges.

Low-Cycle Fatigue Life Prediction

Low-cycle fatigue life predictions were made by the method of universal slopes

from reference 4, which can be expressed by the following equations:

$$\Delta\epsilon_t^L = \Delta\epsilon_e^L + \Delta\epsilon_p^L \tag{2a}$$

$$\Delta\epsilon_e^L = 3.5 \frac{\sigma_u}{E} N_f^{-0.12} \tag{2b}$$

$$\Delta\epsilon_p^L = D^{0.6} N_f^{-0.6} \tag{2c}$$

where

σ_u ultimate tensile strength, MN/m^2

N_f number of fatigue cycles to failure

E elastic modulus, GN/m^2

D tensile ductility, $\ln \frac{100}{100 - RA}$

RA reduction of area, percent

Equation (2b) describes the elastic component of the longitudinal total strain range. For higher cyclic fatigue lives it becomes the dominant quantity. For any fixed cyclic life it varies as the ratio of the material tensile properties σ_u/E varies.

Equation (2c) describes the plastic component of longitudinal total strain range. It becomes the dominant quantity at the lower cyclic fatigue lives. For any fixed cyclic life it varies with tensile ductility of the material to the 0.6 power.

The values of tensile properties used to predict a strain-range - fatigue-life curve for each material at each of the environmental test temperatures were those determined from tensile tests at the same temperature.

RESULTS AND DISCUSSION

Mechanical and Tensile Properties

Mechanical properties of the 10 materials investigated are summarized in table III. Some of these results are also presented in bar graph form in figures 6 to 8. Figure 6 shows that the ultimate tensile strength increased with decreasing temperature for all the materials investigated. The highest initial ultimate tensile strength, that of the 18-percent-nickel maraging steel, increased 35 percent with decreasing temperature to 4 K. But the lowest initial ultimate tensile strength, that of OFHC copper, had a

103 percent increase with decreasing temperature. The greatest increase with decreasing temperature was 182 percent for AISI 304L stainless steel.

The trend of a slight increase in the elastic modulus with decreasing cryogenic temperature for most of the 10 materials investigated is illustrated in figure 7.

The effect of decreasing temperature on ductility is shown in figure 8. Ductility decreased with decreasing temperature for all but two of the materials. The ductility for 2219-T851 aluminum increased significantly with decreasing temperature from room temperature to that of liquid nitrogen. Although its ductility then decreased slightly with a further decrease in temperature to that of liquid helium, it was still greater than at room temperature. For Inconel 718 ductility increased slightly with decreasing temperature from room temperature to that of liquid nitrogen, but it decreased significantly with the decrease in temperature from liquid nitrogen to liquid helium.

There did not appear to be any significant trends in the variations of Poisson's ratio with decreasing temperature for any of the materials investigated. These values ranged from 0.27 to 0.34.

Fatigue Behavior

Results from strain-cycling fatigue tests on the 10 materials investigated at the three different temperatures are summarized in table IV. Long-life load cycling fatigue tests are noted in the table.

Effect of cryogenic temperature on fatigue behavior. - Plots of total longitudinal strain range against experimental cyclic fatigue life are presented in figure 9 for each material and environmental test temperature. The plots show that for the lower cyclic strain ranges (higher cyclic lives) the fatigue resistance of all 10 materials investigated improved with decreasing cryogenic temperature. The observed trend of the temperature effect on fatigue resistance is consistent with what might be expected by using the Manson method of unive sal slopes. This effect is evident from equation (2b). For high cyclic fatigue lives the elastic component of total strain range is dominant and varies as σ_u/E increases with decreasing temperature, thus predicting a higher fatigue resistance.

For the higher cyclic strain ranges (lower cyclic lives) there is a reversal in fatigue behavior for most of the materials investigated. The general trend is for fatigue resistance to decrease with decreasing temperature (fig. 9). For all the materials investigated, except Inconel 718, the fatigue resistance in liquid helium was generally less than in ambient air, and for a majority of the materials the fatigue resistance in liquid helium was less than that in liquid nitrogen at the lower cyclic lives. For Inconel 718, the fatigue resistance increased with decreasing temperature over the entire span of strain range investigated. For AISI 310 stainless steel and 2219-T851 and 2014-T6 aluminum

the fatigue resistance increased in liquid nitrogen over that in ambient air at room temperature over the entire span of strain range investigated. However, in liquid helium there was a crossover and the fatigue resistance became lower at the higher strain ranges (lower cyclic lives) than in liquid nitrogen and ambient air.

The Manson method of universal slopes would be expected to predict decreasing fatigue resistance with decreasing temperature at low cyclic fatigue life, where the plastic strain component is the dominant quantity for materials whose ductility decreases with decreasing temperature. This becomes evident from equation (2c), where the plastic strain range varies with tensile ductility to the 0.6 power. A good example is the fatigue behavior of 18-percent-nickel, maraging steel (300 grade) shown in figure 9. The large drop in fatigue resistance in liquid helium at lower cyclic lives can be attributed to the large drop in tensile ductility of this material in liquid helium.

Comparison of experimental with predicted fatigue behavior. - Comparison of observed experimental fatigue behavior with that predicted by the Manson method of universal slopes is presented in figure 10. Nearness of a data point to the 45° line is a measure of how well the Manson method of universal slopes can predict the experimental data. The dot symbols represent the data from previous research on 29 different materials tested in ambient air (ref. 4). It can be seen that all the data from the present investigation fall well within the scatterband of the earlier data from reference 4. Eighty percent of the fatigue data generated at cryogenic temperatures in this investigation fall within a predicted life factor of 3, as shown by figure 10. It is clearly evident from these results that the Manson method of universal slopes can therefore be used to predict the fatigue behavior of materials at cryogenic temperatures, as well as at room temperature, when the material tensile properties used are determined at the same temperature for which the fatigue resistance predictions are to be made.

SUMMARY OF RESULTS

The strain-cycling fatigue behavior of 10 different alloys and metals (two aluminum alloys, two titanium alloys, two stainless steels, a maraging steel, a high-nickel alloy, pure nickel, and pure copper) was obtained in liquid nitrogen (78 K) and in liquid helium (4 K). Their fatigue behavior was also obtained in ambient air at room temperature (300 K) for purposes of comparison. The major results are summarized as follows:

1. At high cyclic fatigue lives, where the elastic component of strain range is dominant, fatigue resistance increased with decreasing temperature for all the materials investigated.

2. Conversely, at low-cyclic fatigue lives, where the plastic component of strain range is dominant, fatigue resistance decreased with decreasing temperature for most

of the materials investigated. Only for Inconel 718 did the fatigue resistance increase with decreasing temperature over the entire life range investigated.

3. The Manson method of universal slopes can be used to predict the strain-cycling fatigue behavior of these materials at cryogenic temperatures with a degree of accuracy as good as that achieved in an earlier investigation conducted at room temperature. In a comparison of experimental with predicted fatigue behavior, 80 percent of the fatigue data generated at cryogenic temperatures in this investigation were predicted within a life factor of 3.

Lewis Research Center,
National Aeronautics and Space Administration,
Cleveland, Ohio, September 19, 1973,
501-21.

APPENDIX - CONVERSION OF THE INTERNATIONAL SYSTEM OF UNITS TO U.S. CUSTOMARY UNITS

The International System of Units (SI) was adopted by the Eleventh General Conference of Weights and Measures in Paris, October 1960. Conversion factors for the units used herein are from reference 5 and are presented in the following table:

Physical quantity	SI unit (a)	Conversion factor (b)	U.S. customary unit
Frequency	hertz (Hz)	1.0	cps
Force	newton (N)	0.2248	lbf
Length	meter (m)	39.37	in.
Stress	newton/meter^2 (N/m^2)	1.45×10^{-7}	ksi = 1000 lbf/in.^{2}
Temperature	kelvin (K)	$^{o}F = \frac{9}{5}(K - 255.4)$	degree Fahrenheit (^{o}F)

[a]Prefixes to indicate multiples of SI units are as follows:

Prefix	Multiple
milli (m)	10^{-3}
centi (c)	10^{-2}
kilo (k)	10^{3}
mega (M)	10^{6}
giga (G)	10^{9}

[b]Multiply value given in SI units by conversion factor to obtain equivalent value in U.S. customary units or apply conversion formula.

REFERENCES

1. Schwartzberg, F. R.; Osgood, S. H.; Herzog, R. G.; and Kiefer, T. F.: Cryogenic Materials Data Handbook (Revised). Martin Co. (AFML-TDR-64-280, AD-609562), Aug. 1968.

2. Nachtigall, Alfred J.; Klima, Stanley J.; and Freche, John C.: Fatigue of Liquid Rocket Engine Metals at Cryogenic Temperatures to -452° F (4° K). NASA TN D-4274, 1967.

3. Feltner, C. E.; and Laird, C.: Cyclic Stress-Strain Response of F.C.C. Metals and Alloys - I. Phenomenological Experiments. Acta Met., vol. 15, no. 10, Oct. 1967, pp. 1621-1632.

4. Manson, S. S.: Fatigue: A Complex Subject - Some Simple Approximations. Experimental Mech., vol. 5, no. 7, July 1965, pp. 193-226.

5. Committee on Metric Practice: ASTM Metric Practice Guide. ASTM Standard E 380-72, 1972.

TABLE I. - CHEMICAL COMPOSITION OF MATERIALS TESTED

Alloying and/or residual elements	Material									
	2014-T6 aluminum	2219-T851 aluminum	OFHC copper	Inconel 718	Nickel 270	18-percent-nickel maraging steel 300 grade	Ti-5Al-2.5Sn	Ti-6Al-4V	304L stainless steel	310 stainless steel
	Content of alloying or residual element[a], wt.%									
Al	Balance	Balance	-------	0.36	-----	0.10	5.0	6.1	------	------
C	--------	----------	-------	.03	0.01	.012	.023	.02	0.02	0.07
Ca	--------	----------	-------	------	-----	.05	------	------	------	------
Co	--------	----------	-------	------	-----	9.08	------	------	------	------
Cr	0.01	----------	-------	18.59	-----	------	------	------	18.50	25.31
Cu	3.9 - 5.0	5.8 - 6.8	99.99	.03	-----	------	------	------	------	.10
Fe	1.0	0.3	-------	18.94	-----	Balance	.16	.07	Balance	Balance
H	--------	----------	-------	------	-----	------	.0133	.0069	------	------
Mg	0.2 - 0.8	.02	-------	------	-----	------	------	------	------	------
Mn	0.4 - 1.2	0.2 - 0.4	-------	.18	-----	.05	------	------	1.78	1.25
Mo	--------	----------	-------	2.96	-----	4.86	------	------	------	.13
N	--------	----------	-------	------	-----	------	.010	.011	------	------
Ni	--------	----------	-------	52.64	99.99	18.51	------	------	9.78	19.91
O	--------	----------	-------	------	-----	------	.086	.124	------	------
P	--------	----------	.0003	------	-----	.003	------	------	.014	.011
S	--------	----------	.0018	.007	-----	.004	------	------	.011	.013
Si	0.5 - 1.2	0.2	-------	.35	-----	.01	------	------	.049	.47
Sn	--------	----------	-------	------	-----	------	2.6	------	------	------
Ti	.15	0.01 - 0.02	-------	.91	-----	.64	Balance	Balance	------	------
V	--------	----------	-------	------	-----	------	------	4.2	------	------
Zn	.25	.10	.0001	------	-----	------	------	------	------	------
Zr	--------	----------	-------	------	-----	.010	------	------	------	------
Cb + Ta	--------	----------	-------	4.98	-----	------	------	------	------	------

[a]Supplied by vendor.

TABLE II. - CONDITION OF MATERIALS BEFORE TESTING

Material	Condition
2014-T6 aluminum	As received
2219-T851 aluminum	As received
OFHC copper	Vacuum annealed at 920 K (1200° F) for 1 hour after specimen fabrication
Inconel 718	Solution annealed at 1340 K (1950° F) for 1 hour, aged at 1000 K (1350° F) for 9 hours, furnace cooled to 920 K (1200° F), and held until total aging was 19 hours
Nickel 270	As received, hot finished
18-Percent-nickel maraging steel (300 grade)	Solution annealed at mill; aged at 750 K (900° F) for 3 hours and air-cooled after rough machining and prior to final finish grinding
Ti-5Al-2.5Sn	As received, vacuum annealed
Ti-6Al-4V	As received, vacuum annealed
AISI 304L stainless steel	As received, solution annealed at mill
AISI 310 stainless steel	As received, annealed at mill and pickled

TABLE III. - MECHANICAL PROPERTIES OF MATERIALS TESTED

Material	Environmental test temperature	Ultimate tensile strength, σ_u, MN/m^2	Elastic modulus, E, GN/m^2	Tensile ductility, D	Poisson's ratio, μ	Yield strength (0.2 percent offset), σ_y, MN/m^2
	Averages of two or three tests					
2014-T6 aluminum	Ambient air (300 K)	534.3	74.4	0.38	0.321	485.4
	Liquid nitrogen (78 K)	593.6	81.8	.26	.337	520.6
	Liquid helium (4 K)	817.0	82.2	016	.335	706.7
2219-T851 aluminum	Ambient air (300 K)	470.2	70.8	0.36	0.313	361.2
	Liquid nitrogen (78 K)	563.9	78.6	.49	.355	413.7
	Liquid helium (4 K)	663.9	82.0	.44	.341	461.3
OFHC copper	Ambient air (300 K)	206.8	113.7	2.0	0.299	30.3
	Liquid nitrogen (78 K)	333.7	116.5	1.96	.358	44.1
	Liquid helium (4 K)	[a]420.5	138.5	1.8	.334	47.6
Inconel 718	Ambient air (300 K)	1304.0	204.1	0.50	0.308	1110.1
	Liquid nitrogen (78 K)	1514.8	212.3	.51	.307	1285.2
	Liquid helium (4 K)	1848.5	210.9	.35	.297	1372.1
Nickel 270	Ambient air (300 K)	366.1	206.8	2.4	0.310	173.1
	Liquid nitrogen (78 K)	492.9	222.7	2.1	.310	219.3
	Liquid helium (4 K)	734.3	224.0	1.53	.303	225.5
18-Percent-nickel maraging steel (300 grade)	Ambient air (300 K)	1982.2	189.6	0.79	0.314	1903.0
	Liquid nitrogen (78 K)	2475.2	194.3	.51	.307	2344.2
	Liquid helium (4 K)	2688.9	196.4	.047	.312	2318.7
Ti-5Al-2.5Sn	Ambient air (300 K)	863.9	119.2	0.60	0.289	826.0
	Liquid nitrogen (78 K)	1344.4	126.2	.42	.287	1098.3
	Liquid helium (4 K)	1474.1	128.9	.37	.287	1414.1
Ti-6Al-4V	Ambient air (300 K)	1008.7	109.2	0.60	0.333	951.5
	Liquid nitrogen (78 K)	1572.0	118.2	.45	.327	1517.5
	Liquid helium (4 K)	1861.6	119.6	.14	.311	1789.2
AISI 304L stainless steel	Ambient air (300 K)	572.2	190.2	1.56	0.270	276.5
	Liquid nitrogen (78 K)	1427.2	205.1	98	.290	211.7
	Liquid helium (4 K)	1619.6	201.3	.75	308	272.3
AISI 310 stainless steel	Ambient air (300 K)	592.0	143.7	1.35	0.287	230.3
	Liquid nitrogen (78 K)	1107.9	205.5	1.10	303	512.3
	Liquid helium	1317.6	205.5	.90	.296	730.2

[a]Obtained with hourglass-shaped fatigue specimens.

TABLE IV. - SUMMARY OF FATIGUE DATA

Material	Environmental test temperature	Fatigue life, N_f, cycles	Diametral total strain range, $\Delta\epsilon_t^D$	Stress range at half-life, $\Delta\sigma$, MN/m^2	Longitudinal elastic strain range, $\Delta\epsilon_e^L$	Longitudinal plastic strain range, $\Delta\epsilon_p^L$	Longitudinal total strain range, $\Delta\epsilon_t^L$
2014-T6 aluminum	Ambient air (300 K)	11	0.040	1183.8	0.0159	0.0698	0.0857
		40	.020	1154.8	.0155	.0300	.0455
		112	.012	1104.5	.0148	.0145	.0293
		115	.012	1106.6	.0149	.0144	.0293
		230	.009	1065.2	.0143	.0088	.0231
		665	.006	1010.1	.0134	.0034	.0168
		16 520	.003	750.1	.0101	------	.0101
		74 060	.002	556.1	.0075	------	.0075
		77 200	.002	532.9	.0072	------	.0072
	Liquid nitrogen (78 K)	31	0.024	1432.7	0.0176	0.0361	0.0537
		165	.010	1342.7	.0165	.0089	.0254
		1 180	.006	1210.7	.0149	.0019	.0168
		19 430	.004	1068.0	.0131	------	.0131
		43 000	(a)	896.3	.0110	------	.0110
	Liquid helium (4 K)	10	0.030	1854.7	0.0226	0.0529	0.0755
		23	.020	1799.5	.0218	.0254	.0472
		124	.010	1572.0	.0192	.0072	.0264
		2 600	.006	1454.8	.0177	------	.0177
		14 880	(a)	1241.0	.0151	------	.0151
		24 410	(a)	1103.2	.0134	------	.0134
		71 030	(a)	1018.7	.0124	------	.0124
2219-T851 aluminum	Ambient air (300 K)	78	0.025	919.1	0.0129	0.0419	0.0548
		201	.015	832.9	0117	0227	.0344
		344	.0125	803.9	.0113	.0179	.0292
		2 390	.0050	660.5	.0093	.0042	.0135
		13 130	.0030	552.9	.0078	.0011	.0089
		18 410	.0025	515.7	.0073	.0005	.0078
		60 000	.0020	426.1	.0060	.0002	.0062
		68 940	.0020	416.4	.0059	.0003	.0062
	Liquid nitrogen (78 K)	91	0.025	1170.0	0.0149	0.0394	0.0543
		667	.010	976.9	.0124	.0112	.0236
		4 540	.005	818.4	.0104	.0026	.0130
		199 070	(a)	576.0	.0073	------	.0073
	Liquid helium (4 K)	187	0.015	1320.3	0.0161	0.0190	0.0351
		730	.010	1207.9	.0147	.0100	.0247
		10 200	.005	1018.7	.0124	.0015	.0139
		70 760	(a)	843.2	.0103	------	.0103
OFHC copper	Ambient air (300 K)	90	0.030	538.5	0.0047	0.0572	0.0619
		174	.025	514.7	.0045	.0473	.0515
		860	.010	404.0	.0036	.0179	.0215
		3 430	.005	344.0	.0030	.0082	.0112
		14 290	.0025	276.5	.0024	.0036	.0060
		63 250	.0015	210.3	.0018	.002	.0038
	Liquid nitrogen (78 K)	89	0.025	818.7	0.0070	0.0450	0.0520
		182	.020	711.5	.0061	.0356	.0417
		2 150	.010	630.8	.0054	.0161	.0215
		18 750	.005	508.8	.0044	.0069	.0113
		33 900	.004	455.7	.0039	.0052	.0091
		211 120	.002	363.3	.0031	.0018	.0049
	Liquid helium (4 K)	159	0.020	996.9	0.0072	0.0352	0.0424
		377	.015	863.2	.0062	.0258	.0320
		2 490	.010	770.8	0056	.0163	.0219
		9 470	.008	727.4	0052	.0125	.0177
		45 590	.004	548.8	.0040	.0054	.0094
		91 570	.003	524.7	.0038	.0035	.0073

[a] Load cycled.

TABLE IV. - Continued. SUMMARY OF FATIGUE DATA

Material	Environmental test temperature	Fatigue life, N_f, cycles	Diametral total strain range, $\Delta\epsilon_t^D$	Stress range at half-life, $\Delta\sigma$, MN/m^2	Longitudinal elastic strain range, $\Delta\epsilon_e^L$	Longitudinal plastic strain range, $\Delta\epsilon_p^L$	Longitudinal total strain range, $\Delta\epsilon_t^L$
Inconel 718	Ambient air (300 K)	61	0.040	2847.5	0.0139	0.0714	0.0853
		61	.040	2806.1	.0137	.0715	.0852
		292	.020	2468.3	.0121	.0325	.0446
		303	.020	2385.6	0117	.0328	.0445
		1 080	.008	2199.4	.0108	.0094	.0202
		1 460	.008	2092.5	.0103	.0097	0200
		4 000	.004	1834.0	.0090	0025	.0115
		4 000	.004	1834.0	.0090	.0025	.0115
		4 790	.004	1827.1	.0090	.0025	.0115
		5 830	.003	1799.5	.0088	.0006	.0094
		24 440	.002	1461.7	.0072	------	.0072
		86 370	.002	1420.3	.0070	------	.0070
	Liquid nitrogen (78 K)	81	0.040	3612.8	0.0170	0.0696	0.0860
		283	.020	3233.6	.0152	.0307	.0459
		2 240	.008	2261.5	.0077	.0112	.0189
		10 130	.004	2523.5	.0119	.0007	.0126
		167 720	.002	1654.7	.0078	------	.0078
	Liquid helium (4 K)	104	0.040	3819.7	0.0163	0.0703	0.0866
		442	.020	3323.3	.0157	.0307	.0464
		2 790	.008	3054.4	.0145	.0074	.0219
		50 680	(a)	2526.9	.0120	------	.0120
Nickel 270	Ambient air (300 K)	187	0.025	861.8	0.0041	0.0474	0.0515
		1 110	.010	718.4	.0032	.0180	.0212
		2 580	.005	638.4	.0031	.0081	.0112
		75 280	.001	359.9	.0017	.0009	.0026
	Liquid nitrogen (78 K)	140	0.025	1469.2	0.0066	0.0459	0.0525
		3 600	.005	932.2	.0042	.0074	.0116
		25 740	.002	722.6	0032	.0020	.0052
		273 330	.001	631.5	.0028	.0002	.0030
	Liquid helium (4 K)	191	0.015	1538.2	0.0069	0.0258	0.0327
		614	.0125	1465.1	.0065	.0210	.0275
		736	.010	1418.9	.0063	.0162	.0225
		4 250	.005	1168.6	.0052	.0068	.0120
		21 180	.0025	1065.2	.0048	.0021	.0069
		67 170	.0015	986.6	.0044	.0003	.0047
18-Percent-nickel maraging steel (300 grade)	Ambient air (300 K)	91	0.040	3447.4	0.0186	0.0688	0.0874
		196	.030	3185.4	.0171	.0486	.0657
		436	.020	3050.9	.0164	.0301	.0465
		1 170	.010	2640.6	.0142	.0126	.0268
		3 240	.005	2541.4	.0137	.0035	.0172
		19 550	.0035	2171.8	.0117	.0001	.0118
		21 960	.0035	2109.8	.0113	.0003	.0116
		21 300	(a)	------	.0110	------	.0112
	Liquid nitrogen (78 K)	84	0.030	4812.5	0.0249	0.0450	0.0699
		265	.020	3902.4	.0202	.0279	.0481
		704	.0094	4171.3	.0216	.0058	.0274
		1 150	.010	3547.4	.0184	.0090	.0274
		1 330	.0075	3866.6	.0200	.0030	.0230
		4 500	.005	3295.7	.0171	------	.0171
		8 700	.005	3226.7	.0167	------	.0167
		14 400	.004	2840.6	.0147	------	.0147
		28 360	(a)	2094.6	.0108	------	.0108
		88 660	(a)	2178.7	.0113	------	.0113
	Liquid helium (4 K)	19	0.0125	5257 3	0.0268	0.0083	0.0351
		60	.01	5047.0	.0257	.0040	.0297
		146	.0075	4722.9	.0240	------	.0240
		155	.01	4681.5	.0238	.0051	.0289
		1 960	.005	3400.5	.0173	------	.0173
		72 280	(a)	2240.8	.0114	------	.0114

[a] Load cycled.

TABLE IV. - Continued. SUMMARY OF FATIGUE DATA

Material	Environmental test temperature	Fatigue life, N_f, cycles	Diametral total strain range, $\Delta\epsilon_t^D$	Stress range at half-life, $\Delta\sigma$, MN/m^2	Longitudinal elastic strain range, $\Delta\epsilon_e^L$	Longitudinal plastic strain range, $\Delta\epsilon_p^L$	Longitudinal total strain range, $\Delta\epsilon_t^L$
Ti-5Al-2.5Sn	Ambient air (300 K)	53	0.050	1827.1	0.0153	0.0911	0.1064
		133	.030	1678.9	.0140	.0519	.0659
		207	.020	1641.3	.0137	.0323	.0460
		415	.014	1576.9	.0132	.0203	.0335
		968	.008	1559.6	.0131	.0084	.0215
		2 200	.0048	1385.8	.0116	.0029	.0145
		2 600	.0048	1434.1	.0120	.0027	.0147
		2 930	.0056	1406.5	.0118	.0044	.0162
		4 410	.004	1339.0	.0112	.0015	.0127
		5 240	.004	1369.3	.0115	.0014	.0129
		15 540	.0032	1266.6	.0106	.0003	.0109
	Liquid nitrogen (78 K)	43	0.040	3088.9	0.0245	0.0659	0.0904
		126	.018	2737.2	.0217	.0235	.0452
		263	.0112	2585.5	.0205	.0106	.0311
		382	.014	2592.4	.0206	.0162	.0368
		515	.014	2528.3	.0200	.0165	.0365
		1 230	.008	2444.9	.0194	.0049	.0243
		10 580	.0048	2141.5	.0175	------	.0175
		38 360	.004	1703.0	.0135	.0002	.0137
		60 800	.004	1754.7	.0139	------	.0139
	Liquid helium (4 K)	52	0.040	3392.2	0.0263	0.0649	0.0912
		128	.020	3025.4	.0235	.0265	.0500
		275	.020	3171.6	.0246	.0259	.0505
		934	.010	2933.7	.0229	.0069	.0297
		3 990	.006	2644.8	.0205	.0002	.0207
		6 720	.005	1892.6	.0147	.0016	.0163
		64 510	(a)	1837.5	.0143	------	.0143
Ti-6Al-4V	Ambient air (300 K)	85	0.040	1975.3	0.0180	0.0680	0.0860
		103	.030	1956.0	.0178	.0481	.0659
		259	.020	1896.1	.0173	.0285	.0458
		717	.010	1760.9	.0161	.0093	.0254
		720	.010	1745.8	.0159	.0094	.0253
		1 770	.006	1642.3	.0153	.0018	.0171
		2 210	.0061	1596.1	.0146	.0028	.0174
		2 720	.0060	1678.9	.0153	.0018	.0171
		3 300	.0060	1661.6	.0152	.0019	.0171
		3 700	.0060	1668.5	.0152	.0019	.0171
		10 720	.004	1410.7	.0129	------	.0129
		61 460	(a)	1123.8	.0103	------	.0103
	Liquid nitrogen (78 K)	47	0.020	3392.2	0.0286	0.0213	0.0499
		254	.015	3171.6	.0267	.0125	.0392
		313	.012	3061.2	.0258	.0071	.0329
		509	.008	2954.4	.0249	------	.0249
		2 050	.006	2726.9	.0230	------	.0230
		8 410	.006	2490.4	.0210	------	.0210
		25 800	.005	2271.8	.0192	------	.0192
		34 030	.005	2047.7	.0173	------	.0173
	Liquid helium (4 K)	82	0.020	3681.8	0.0307	0.0209	0.0516
		181	.012	3602.5	.0300	.0053	0353
		625	.0102	3636.9	.0299	.0018	.0307
		720	.008	3454.3	.0288	------	.0288
		877	.008	3636.9	.0303	------	.0303
		2 660	.006	2591.0	0216	------	.0216
		3 170	.006	2447.6	.0204	------	.0204
		21 460	.004	2466.9	.0148	------	.0148

(a) Load cycled.

TABLE IV. - Concluded. SUMMARY OF FATIGUE DATA

Material	Environmental test temperature	Fatigue life, N_f, cycles	Diametral total strain range, $\Delta\epsilon_t^D$	Stress range at half-life, $\Delta\sigma$, MN/m^2	Longitudinal elastic strain range, $\Delta\epsilon_e^L$	Longitudinal plastic strain range, $\Delta\epsilon_p^L$	Longitudinal total strain range, $\Delta\epsilon_t^L$
AISI 304L stainless steel	Ambient air (300 K)	130	0.020	1447.9	0.0076	0.0359	0.0435
		295	.015	1194.5	.0063	.0266	.0329
		555	.010	966.6	.0051	.0173	.0224
		3 030	.005	635.7	.0033	.0082	.0115
		3 580	.005	650.2	.0034	.0082	.0116
		4 230	.005	580.5	.0031	.0084	.0115
		44 010	.0025	489.5	.0026	.0036	.0062
		994 880	.001	429.2	.0022	.0008	.0030
	Liquid nitrogen (78 K)	132	0.020	2792.4	0.0136	0.0321	0.0457
		184	.015	3240.5	.0158	.0209	.0367
		453	.010	3057.8	.0149	.0114	.0263
		2 830	.005	2358.0	.0115	.0033	.0148
		20 440	.0025	1616.8	.0079	.0004	.0083
		42 960	.0025	1435.5	.0070	.0009	.0079
		157 990	.0020	1073.5	.0052	.0010	.0062
	Liquid helium (4 K)	228	0.0125	3385.3	0.0168	0.0146	0.0314
		414	.010	3257.8	.0162	.0100	.0262
		2 920	.005	2238.0	.0111	.0032	.0143
		38 640	.0025	1447.9	.0072	.0006	.0078
AISI 310 stainless steel	Ambient air (300 K)	87	0.040	1511.3	0.0078	0.0755	0.0833
		438	.014	1065.2	.0055	.0268	.0323
		1 300	.010	948.7	.0049	.0172	.0221
		5 240	.005	710.2	.0037	.0079	.0116
		5 660	.005	682.6	.0035	.0080	.0115
		35 580	.0025	579.2	.0030	.0033	.0063
		43 710	.0025	524.0	.0027	.0034	.0061
		620 000	.00125	439.5	.0023	.0012	.0035
	Liquid nitrogen (78 K)	147	0.050	2195.3	0.0107	0.0934	0.1041
		412	.025	1918.1	.0093	.0442	.0535
		607	.020	1554.8	.0076	.0353	.0429
		1 010	.015	1658.2	.0081	.0250	.0331
		2 530	.010	1259.7	.0061	.0162	.0223
		15 200	.005	1123.8	.0055	.0066	.0121
		117 300	.0025	1058.3	.0052	.0018	.0070
		230 940	.002	904.6	.0044	.0013	.0057
		570 590	.002	921.8	.0044	.0013	.0057
	Liquid helium (4 K)	47	0.05	2415.9	0.0118	0.0930	0.1048
		350	.03	2027.1	.0099	.0542	.0641
		2 020	.015	1675.4	.0082	.0252	.0334
		3 690	.010	1589.2	.0077	0154	.0231
		55 900	.005	1174.2	.0057	.0066	.0123

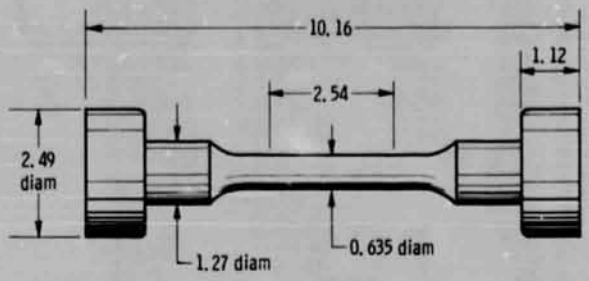

(a) Tensile specimen.

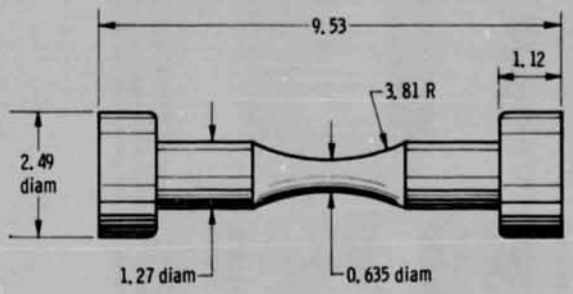

(b) Fatigue specimen.

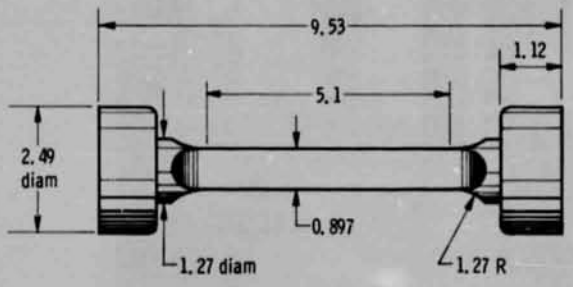

(c) Specimen for determining elastic constants.

Figure 1. - Specimen geometry. Dimensions are in centimeters.

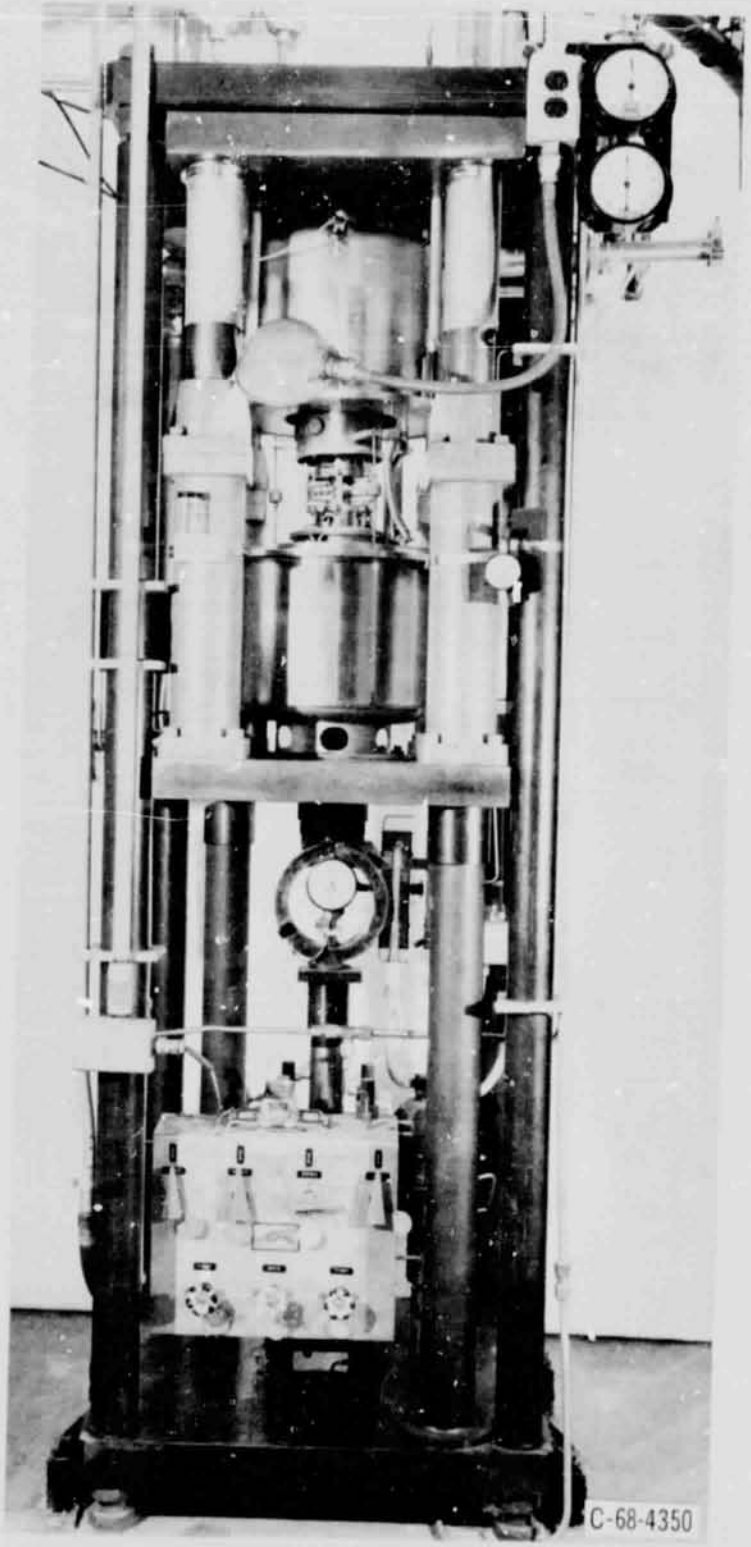

Figure 2. - Push-pull fatigue testing machine with cryostat.

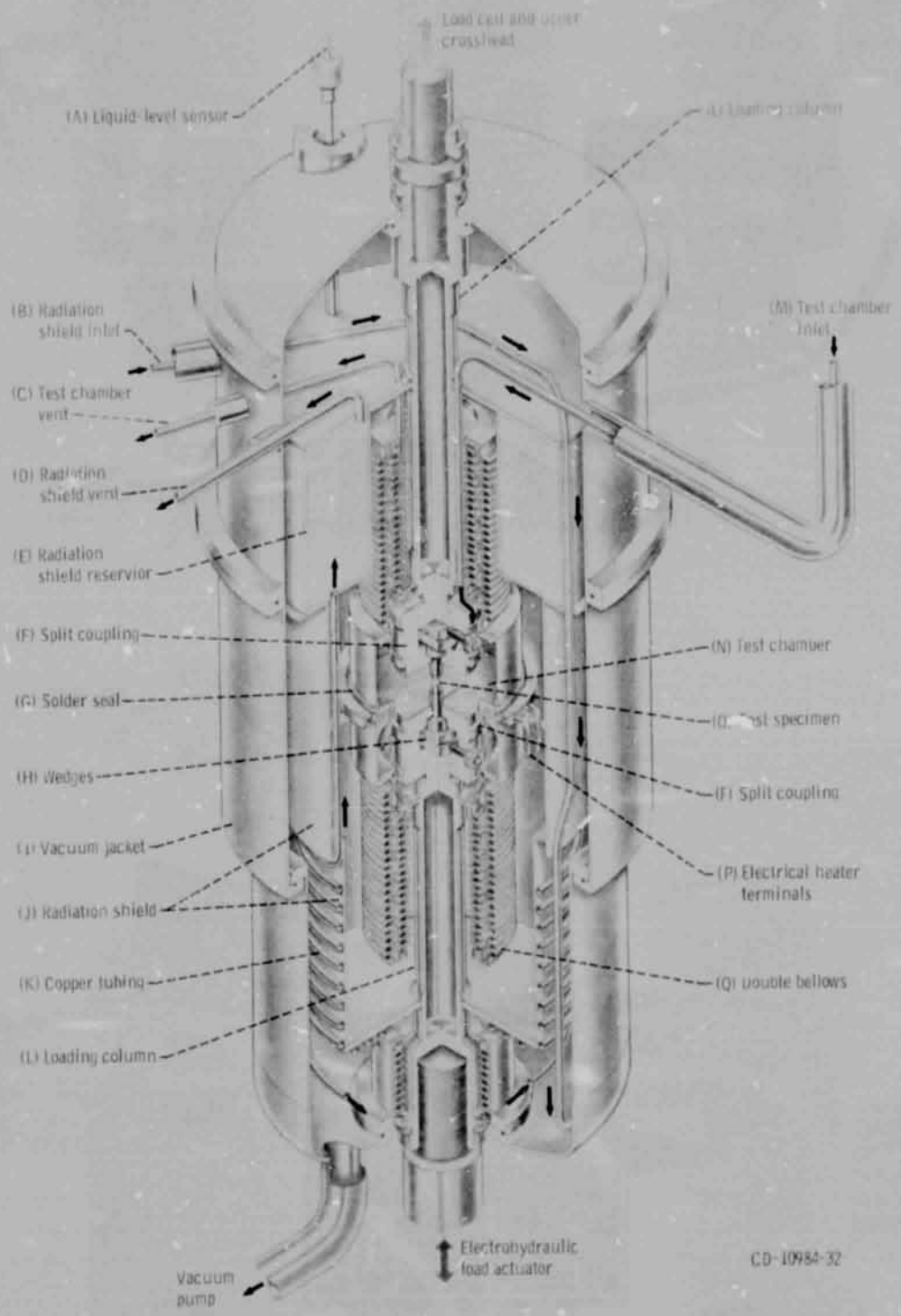

Figure 3. - Cryostat for tensile and fatigue testing.

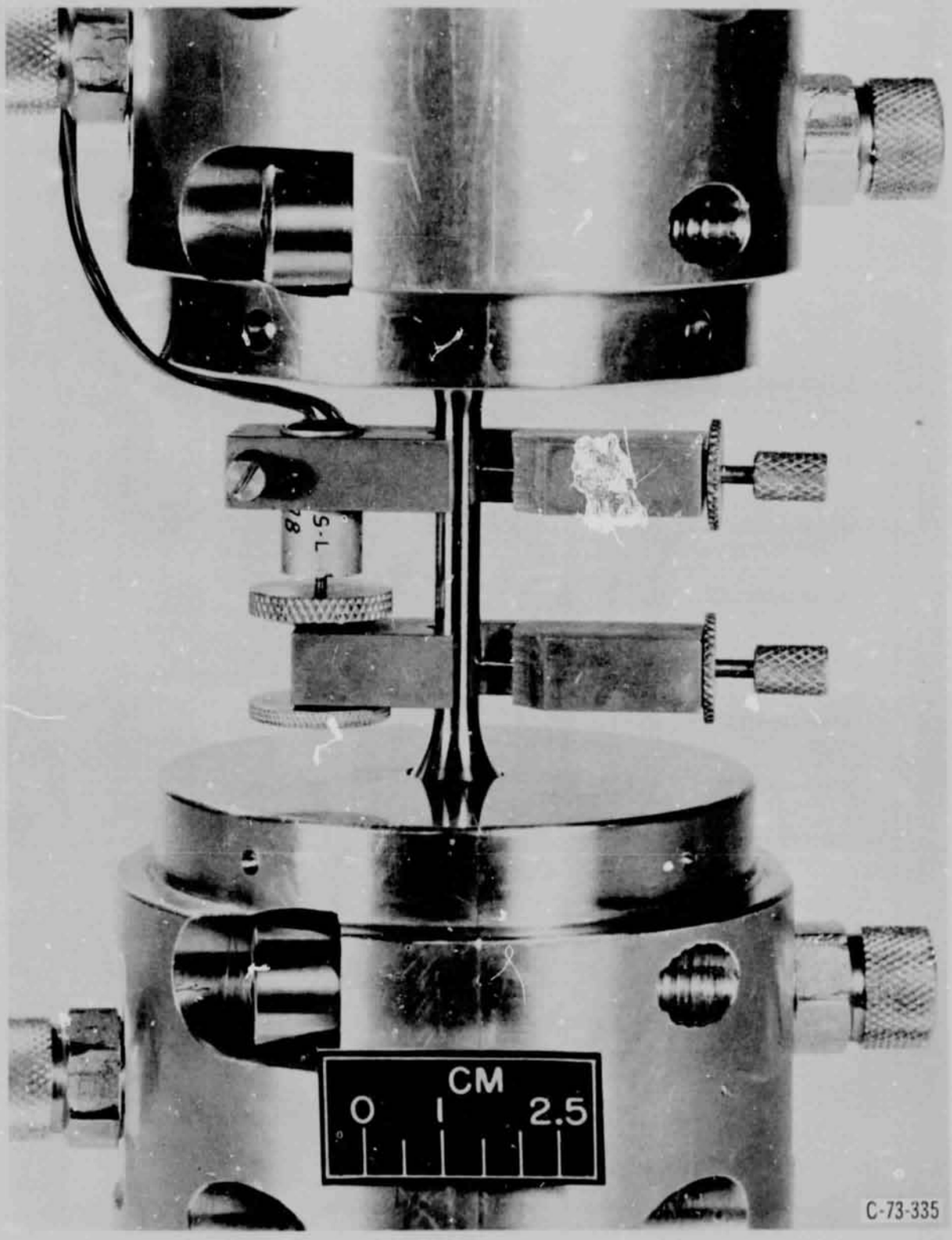

Figure 4. - Extensometer used with tensile tests in liquid helium.

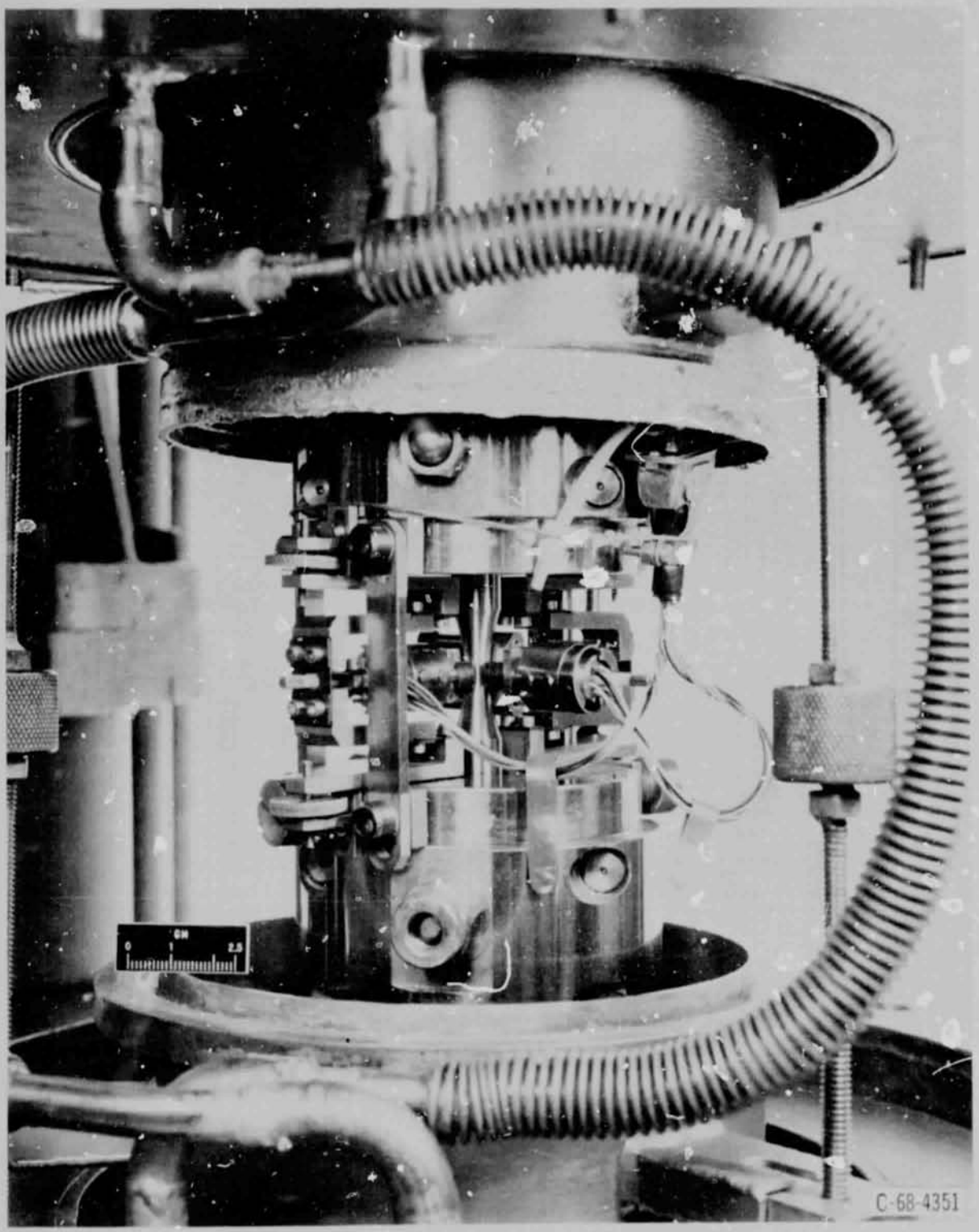

Figure 5. - Diametral extensometer used for strain-cycling fatigue tests, shown mounted on test specimen in specimen chamber.

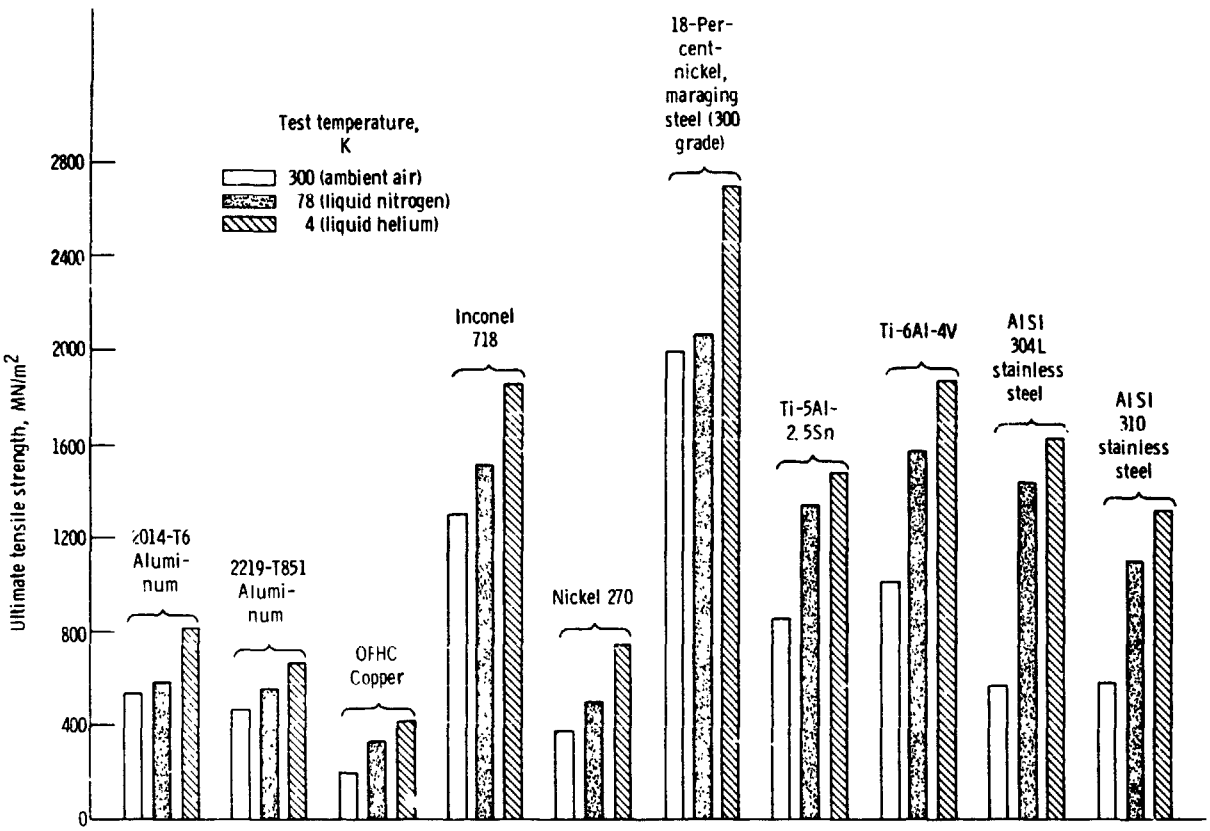

Figure 6. - Effect of cryogenic temperature on ultimate tensile strength of materials investigated.

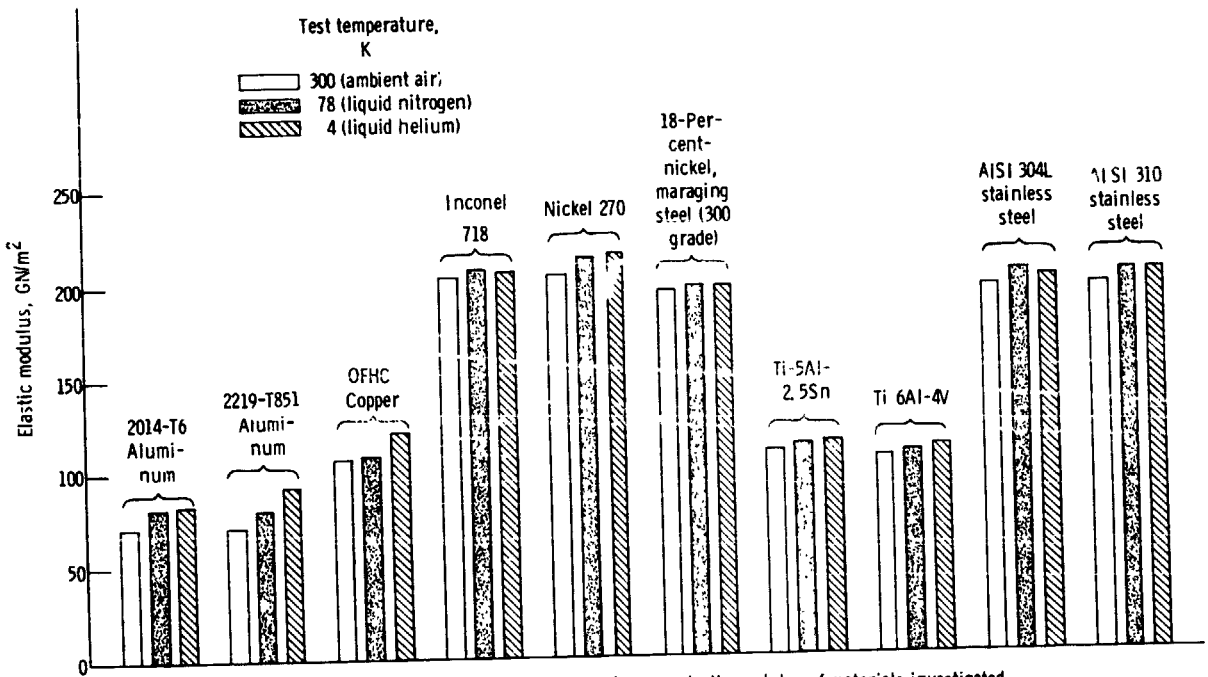

Figure 7. - Effect of cryogenic temperature on elastic modulus of materials investigated.

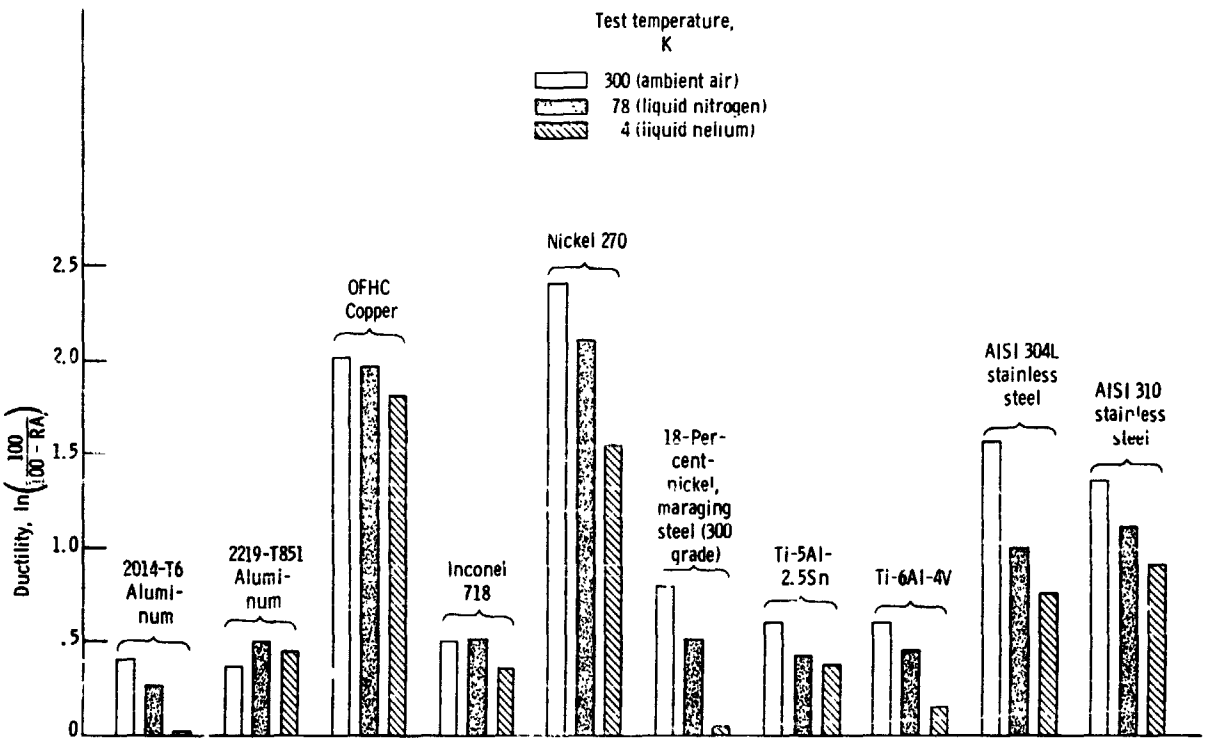

Figure 8. - Effect of cryogenic temperature on ductility of materials investigated.

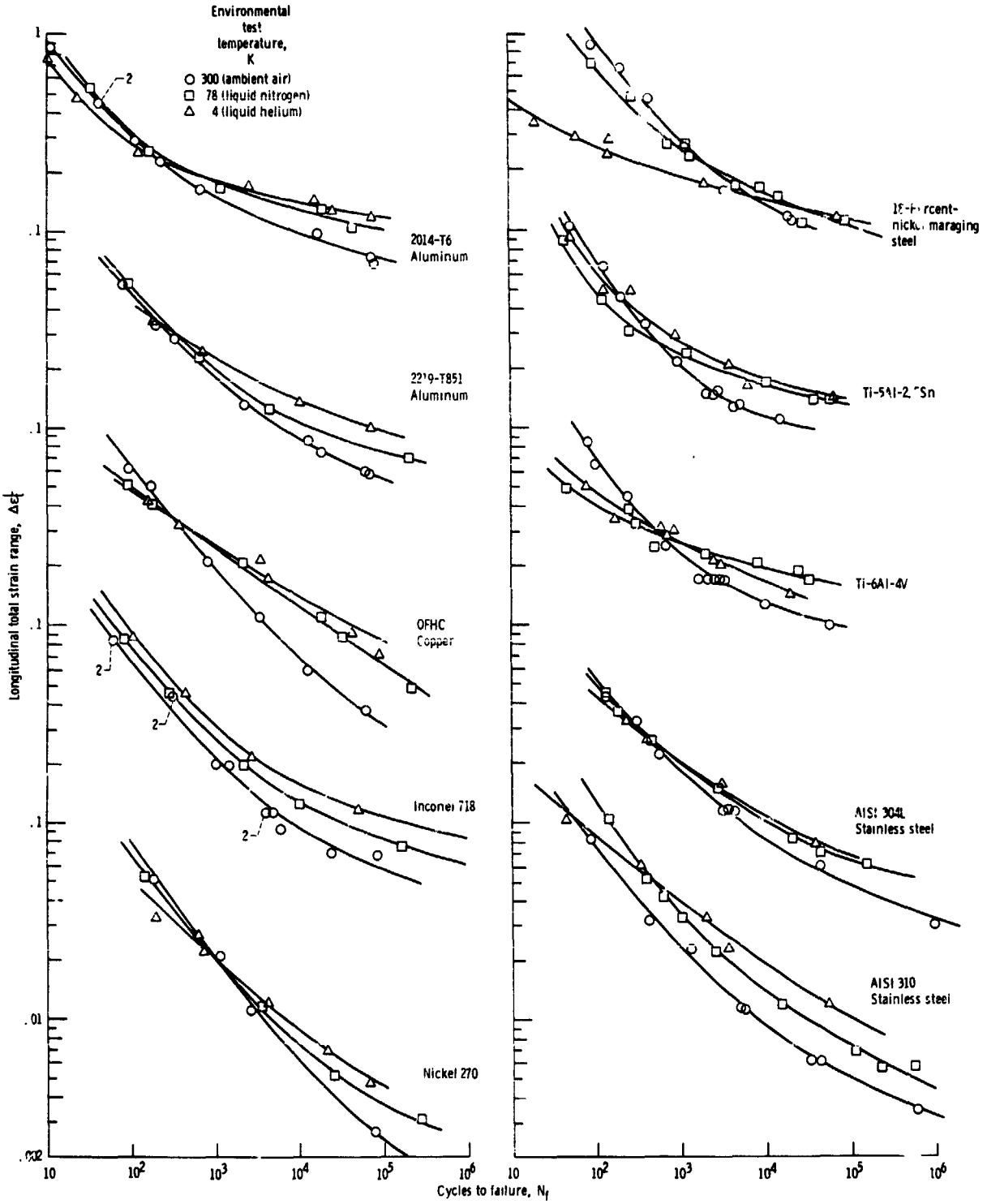

Figure 9. - Effect of test temperature on fatigue behavior of 10 strain-cycled structural metals.

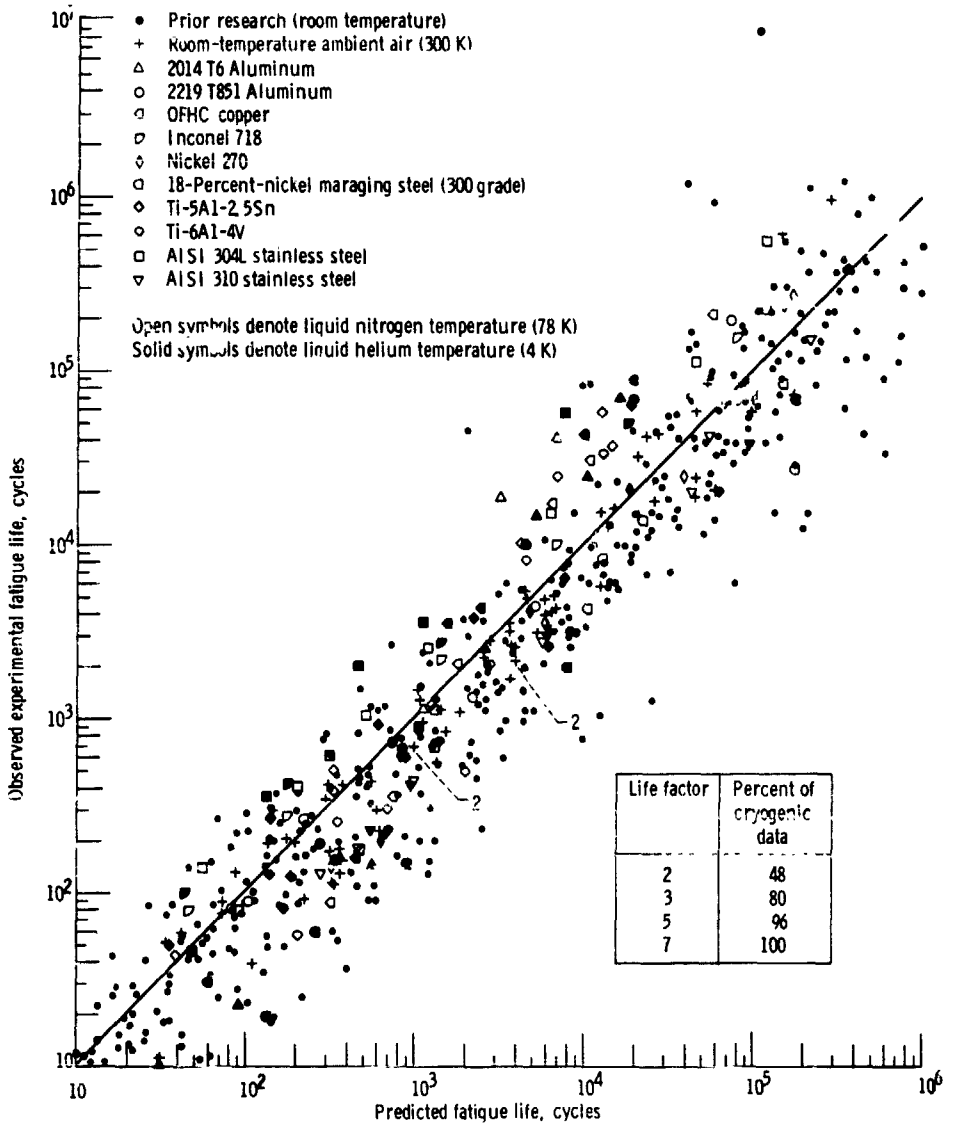

Figure 10. - Verification of life prediction at cryogenic temperatures for 10 materials by the Manson method of universal slopes.